# Development and experimentation of a new MPPT synergetic control for photovoltaic systems

H. ATTOUI[a], F. KHABER[a], M. MELHAOUI[b], K. KASSMI[b], N. ESSOUNBOULI[c]
[a]*QUERE Laboratory, Faculty of technology, University of Setif 1, 19000 Setif, Algeria*
[b]*LETAS Laboratory, Faculty of Science, University Mohamed the First, Oujda 60000, Morocco*
[c]*CReSTIC Laboratory, University of Reims Champagne Ardennes. IUT de Troyes, 9 rue de Quebec B.P. 396, 10026 Troyes, France*

This paper proposes a new approach of maximum power point tracking (MPPT) using a synergetic control (SC) theory for photovoltaic (PV) system. This system is mainly composed of a solar array, DC/DC boost converter, MPPT controller, and an output load. Synergetic controller is used for boost converter to achieve the maximum power output. The stability of the closed-loop system is guaranteed using Lyapunov's method. The new approach gives a good maximum power operation under different conditions such as changing solar radiation and PV cell temperature. To show the validity and robustness of the proposed approach, different simulations under different atmospheric conditions are realized using Matlab/Simulink. The implementation of synergetic control is also presented. The experimental results show satisfactory performance of the proposed approach.

(Received September 16, 2014; accepted February 10, 2016)

*Keywords***:** Synergetic control, Maximum power point tracking, Robustness, Photovoltaic system

## 1. Introduction

Renewable energy resources will be an increasingly important part of power generation in the new millennium. The importance of photovoltaic generation is greater nowadays as a renewable source since it exhibits many merits such as cleanness, little maintenance and no noise [1].

All PV systems have two big problems that the efficiency of electric-power generation is very low, especially under low-irradiation states, and the amount of the electric power generated by solar arrays is always changing with weather conditions. Load mismatch occurs under these weather varying conditions such that maximum power is not extracted and delivered to the load. This issue constitutes, the so-called maximum power point tracking (MPPT) problem.

In recent years, a large number of techniques have been proposed for tracking the maximum power point. Fractional open-circuit voltage and short-circuit current [2, 3] strategies provide a simple and effective way to acquire the maximum power. However, they require periodical disconnection or short-circuit of the PV modules to measure the open-circuit voltage or short-circuit current for reference, resulting in more power loss.

Perturbation and observation (P&O) and hill climbing methods are widely applied in the MPPT controllers due to their simplicity and easy implementation [3-4]. P&O method involves a perturbation in the operating voltage of the PV array, while hill climbing strategy introduces a perturbation in the duty ratio of the power converter [3] and is more attractive due to the simplified control structure [5].

Incremental Inductance (INC) method, which is based on the fact that the slope of the PV array power vs. voltage curve is zero at the MPP, has been proposed to improve the tracking accuracy and dynamic performance under rapidly varying conditions [3, 6].

In [7] and [8] an MPPT using sliding mode current controller for PV system is also proposed, yielding an algorithm principle consisting in varying the load voltage until reach the maximum power.

Furthermore, intelligent methods such as artificial neural networks, genetic algorithms and fuzzy logic have been also adopted to estimate the voltage and the load current values. Thus allowing for the variation of the DC-DC converter duty cycle so as to place the PV system in its MPP at any given S, T, and load conditions [9,10]. For more details on these methods and some related applications on solar energy, PV panel the readers can refer to [9–14] and the references therein.

The general requirements for maximum power point tracking (MPPT) are simplicity and low cost, quick tracking under changing conditions, and small output power fluctuation. The search for a more efficient method to solve this problem is ongoing quest.

Synergetic control (SC) theory was introduced in general terms by Kolesnikov [15]. Its application to a single boost converter was introduced in [16], and some practical aspects with reference to both simulations and actual hardware were discussed in [17-19].

This paper proposes a novel approach to track maximum power point using synergetic approach for

photovoltaic system under different atmospheric conditions. The remainder of this paper is organized as follows. Section 2 gives the PV panel model. The synergetic control procedure and MPPT system modeling are exposed in Section 3. The design of synergetic MPPT controller is given in section 4. Section 5 presents the simulation and experimental results. Conclusions are presented in the last section.

## 2. Modeling of a PV cell by Matlab

### 2.1 Equivalent model and characteristic of photovoltaic cell

A PV cell model is shown in Fig.1. Where $I_{ph}$ indicates photocurrent, which depends on the level of light intensity, $I_d$ is current through the diode, $I_{pv}$ (Photovoltaic panel current) is output current, $V_{pv}$ (Photovoltaic panel) voltage is open-circuit voltage, $R_{sh}$ is the equivalent shunt resistance, and $R_s$ is the intrinsic series resistance.

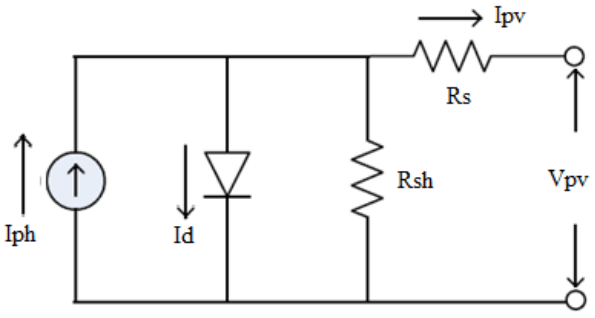


*Fig. 1.Equivalent circuit of PV cell.*

Consequently the nonlinear characteristics of PV cell can be represented by following equation.

$$I_{pv} = I_{ph} - I_0\left[exp\left(\frac{q(V_{pv} + R_s I)}{AK_bT}\right) - 1\right] - \frac{(V_{pv} + R_s I)}{R_{sh}} \quad (1)$$

$$I_{ph} = S/1000(I_{scr} + K_i \times (T - T_r\ )) \quad (2)$$

$$I_0 = I_{rr}\left(\frac{T}{T_r}\right)^3 exp\left(\left[\frac{qEg}{k_bA}\right] \times \left[\left(\frac{1}{T_r}\right) - \left(\frac{1}{T}\right)\right]\right) \quad (3)$$

An ideal PV cell has very low equivalent series resistance $R_s$ and very high equivalent parallel resistance $R_{sh}$, generally speaking for silicon or polysilicon PV cell, in the general engineering application they can be neglected, and equation (1) becomes:

$$I_{pv} = I_{ph} - I_d = I_{ph} - I_0\left[exp\left(\frac{q\,V_{pv}}{AK_bT}\right) - 1\right] \quad (4)$$

where $I_{pv}$ is the output current (A), $V_{pv}$ the voltage (V), $I_0$ is reverse saturation current, $q$ the electronic charge, $K_b$ is Boltzmann's constant, $T$ is ambient temperature in Kelvin, $T_r$ is reference temperature, $I_{rr}$ is the saturation current at the reference temperature, $I_{scr}$ is the short-circuit current of PV cell under standard conditions, $E_g$ is the energy of the band gap for silicon, $A$ is the P-N junction's ideality factor, $K_i$ is the short-circuit-current temperature coefficient, $S$ is solar irradiance ($W/m^2$).

### 2. 2 PV characteristic

The current-to-voltage characteristic of a solar cell is nonlinear, which makes it difficult to determine the MPP.

Fig. 2 illustrates the operating characteristic curves of the solar array under a given irradiance. It consists of two regions: one is the current source region, and the other is the voltage source region. In the voltage source region (on the right side of the curve), the internal impedance of the solar array is low and in the current source region (on the left side of the curve), the internal impedance of the solar array is high. The MPP of the solar array is located at the knee of the curve.

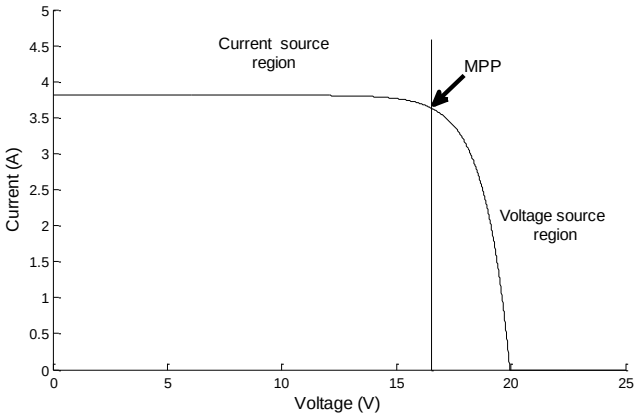


*Fig.2. I-V characteristic.*

The PV characteristic is plotted in Fig. 3 under different irradiance levels, and PV characteristic under different temperatures is plotted in Fig. 4.

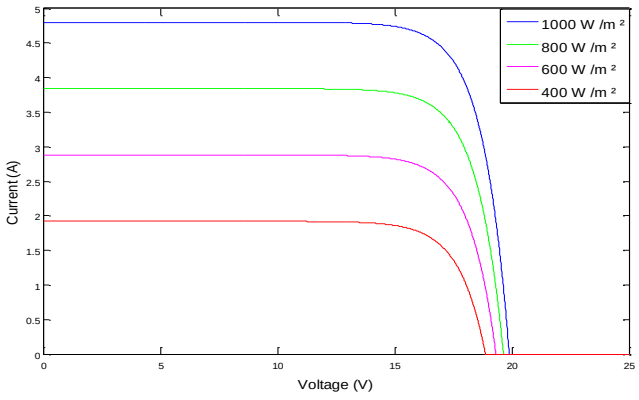


*Fig. 3. PV characteristic under different irradiance levels (temperature =298 K).*

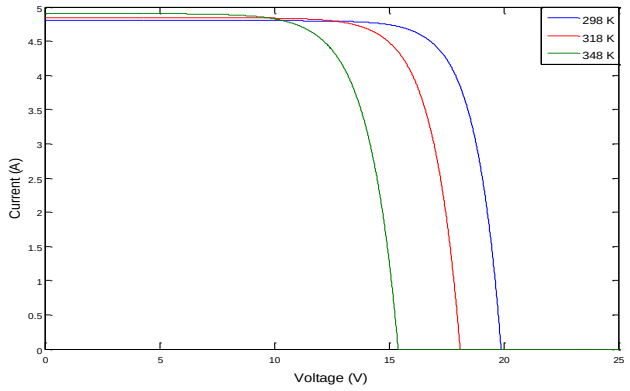


*Fig. 4. PV characteristic under different temperatures (irradiance = 1000 W/m²).*

As illustrated in the figures, the open-circuit voltage ($V_{oc}$) is dominated by temperature, and solar irradiance has preeminent influence on short- circuit current ($I_{sc}$). We can conclude that high temperature and low solar irradiance will reduce the power conversion capability.

## 3. Synergetic control procedure

The synergetic control design procedure follows the Analytical Design of Aggregated Regulators (ADAR) method [17]. The general synergetic procedure is reviewed in this section.

The main steps of the procedure can be summarized as follows.

Suppose the system to be controlled is described by a set of non linear differential equation of the form

$$\frac{dx}{dt} = f(x, d, t) \tag{5}$$

where $x$ is the state variable vector, $d$ is the control input vector and $t$ is time.

Start by defining a macro-variable as a function of the state variables:

$$\Psi = \psi(x, t) \tag{6}$$

The control signal will force the system to operate on the manifold

$$\Psi = 0 \tag{7}$$

The designer can select the characteristics of the macro-variable according to the control specifications (e.g: limitation in the control output, the settling time, and so on). In the trivial case the macro-variable can be a simple linear combination of the state variables. The same process can be repeated, defining as many macro-variables as there are control channels.

The desired dynamic evolution of the macro-variable is:

$$T_S\left(\frac{d\Psi}{dt}\right) + \Psi = 0 \quad ; \qquad T_s > 0 \tag{8}$$

where $T_s$ is design parameter specifying the convergence speed to the manifold specified by the macro-variable equals to zero.

The chain rule of differentiation gives:

$$d\Psi/dt = (d\Psi/dx)(dx/dt) \tag{9}$$

Combining (5), (8), and (9) we obtain

$$T_S(d\Psi/dx)f(x, d, t) + \Psi = 0 \tag{10}$$

Equation (10) is finally used to synthesize the control law $d$.

Upon solving Eq. (10) for $d$, the control law can be found as:

$$d = g(x, t, \Psi(x, t), T_S) \tag{11}$$

From Eq. (11), it can be seen that the control output depends not only on the system state variables, but also on the selected macro-variable and time constant $T_s$. In other words, the designer can choose the characteristic of the controller by selecting a suitable macro-variable and time constant $T_s$.

### 3. 1. MPPT system modeling

Consider a boost type converter connected to a PV module with a resistive load as illustrated in Fig. 5.

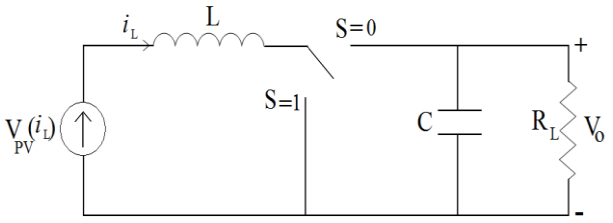


*Fig. 5.MPPT system schematics.*

According to the position of switch S, the system can be written in two sets of state equations. If the switch is in position S = 0, the differential equations can be written as:

$$\frac{di_{L1}}{dt} = \frac{Vpv(i_L)}{L} - \frac{V_0}{L} \tag{12.a}$$

$$\frac{dV_{01}}{dt} = \frac{i_L}{C} - \frac{V_0}{CR_L} \tag{12.b}$$

If the switch is in position S = 1, the differential equations can be expressed as:

$$\frac{di_{L2}}{dt} = \frac{Vpv(iL)}{L} \tag{13.a}$$

$$\frac{dV_{02}}{dt} = -\frac{V_0}{CR_L} \qquad (13.b)$$

By using the state space averaging method [18], Eqs.(12) and (13) can be combined into one set of state equation to represent the dynamic of the system. Based on the idea of Pulse-Width Modulation (PWM), the ratio of the switch in position 1 in a period is defined as duty ratio. Two distinct equation sets are weighted by the duty ratio and superimposed:

$$\frac{dX}{dt} = (1-d)\frac{dX_1}{dt} + d \times \frac{dX_1}{dt} \qquad (14)$$

where $X_1=[i_{L1}\ \ V_{01}]^T$, $X_2=[i_{L2}\ \ V_{02}]^T$, and $d\in[0\ 1]$ is the duty ratio. Hence the dynamic equation of the system can be described by:

$$\frac{di_L}{dt} = -(1-d)\frac{V_0}{L} + \frac{V_{pv}}{L} \qquad (15.a)$$

$$\frac{dV_0}{dt} = (1-d)\frac{i_L}{C} - \frac{V_o}{C\,R_L} \qquad (15.b)$$

where $C$ is the capacity, $L$ is the inductance, $R_L$ is the resistive load, $d\in[0\ 1]$ is the duty ratio, which is also the control input. $V_0$ is the output voltage and $i_L$ is the inductor current. Note that the equivalent series resistance (ESR) of the inductor and wiring resistance are neglected in this case, so $i_L$ is assumed to be equal to the PV current ($I_{PV}$). Eq. (15) can be written in general form of the nonlinear time invariant system.

$$\frac{dX}{dt} = f(X) + g(X)\,d \qquad (16)$$

## 4. Design of synergetic MPPT controller

In this study, we introduce the concept of the synergetic control for the MPPT system.

By selecting the manifold as $\partial P_{PV}/\partial I_{PV} = 0$, it is guaranteed that the system state will hit the manifold and produce maximum power output persistently.

$$\frac{\partial P_{pv}}{\partial I_{pv}} = \frac{\partial I_{pv}^2 R_{pv}}{\partial I_{pv}} = I_{pv}\left(2R_{pv} + I_{pv}\frac{\partial R_{pv}}{\partial I_{pv}}\right) = 0 \qquad (17)$$

Where $R=V_{PV}/I_{PV}$ is the equivalent load connect to the PV, and $I_{PV}$ the PV current which is equal to $i_L$ in this case.

The solution of (17) is $2R_{pv} + I_{pv}\frac{\partial R_{pv}}{\partial I_{pv}} = 0$

Hence, the manifold is defined as:

$$\Psi = 2R_{pv} + i_L\frac{\partial R_{pv}}{\partial i_L} \qquad (18)$$

Then the desired dynamic evolution of the macro-variable can be expressed as:

$$T_s(d\Psi/dx) + \Psi = 0\,; \quad T_S > 0 \qquad (19)$$

Where

$$d\Psi/dt = (d\Psi/dX)(dX/dt) \qquad (20)$$

The substitution of $\Psi'$ from Eq. (20) into the functional equation (19) yields

$$T_s\{(d\Psi/dx_1)\,(f(x) + g(x)\,d(t))\} + \Psi = 0$$

$$(\partial\Psi/\partial X)\,(\frac{V_{pv} - V_0}{L} + \frac{V_0}{L}\,d(t)) = -\Psi/T_s \qquad (21)$$

$$d(t) = 1 - \left(\Psi L/\left(V_0 T_s\frac{\partial\Psi}{\partial X}\right)\right) - \left(\frac{V_{pv}}{V_0}\right) \qquad (22)$$

The time derivative of $\Psi$ can be written as:

$$\frac{\partial\Psi}{\partial X} = 3\,\frac{\partial R_{pv}}{\partial i_L} + i_L\frac{\partial^2 R_{pv}}{\partial i_L^2} \qquad (23)$$

Replacing $R_{pv}$ by the definition of $R_{pv}= V_{pv}/I_{pv}$

$$\frac{\partial R_{pv}}{\partial i_L} = \frac{\partial}{\partial i_L}\left[\frac{Vpv}{i_L}\right] = \frac{1}{i_L}\left(\frac{\partial V_{pv}}{\partial i_L}\right) - \frac{V_{pv}}{{i_L}^2} \qquad (24)$$

$$\frac{\partial^2 R_{pv}}{\partial {i_L}^2} = \frac{1}{i_L}\left(\frac{\partial^2 V_{pv}}{\partial {i_L}^2}\right) - \left(\frac{2}{{i_L}^2}\right)\left(\frac{\partial V_{pv}}{\partial i_L}\right) + \frac{2V_{pv}}{{i_L}^3} \qquad (25)$$

By (4), the PV voltage ($V_{pv}$) can be rewritten as function of PV current ($I_{pv}$)

$$V_{pv} = \left(\frac{K_b TA}{q}\right) ln\left(\frac{I_{ph} + I_0 - I_{pv}}{I_0}\right) \qquad (26)$$

Substituting Eq. (23) into Eq. (22), the synergetic control signal is defined as:

$$d(t) = 1 - \frac{\Psi L}{V_o T_s\left(\frac{3\partial R_{pv}}{\partial i_L} + i_L\frac{\partial^2 R_{pv}}{\partial i_L^2}\right)} - \frac{V_{pv}}{V_o} \qquad (27)$$

Asymptotic stability is obtained using the Lyapunov function candidate:

$$V_L = \frac{1}{2}\Psi^2 \qquad (28)$$

The derivate of $V_L$ is:

$$\frac{dV_L}{dt} = \Psi\left(\frac{d\Psi}{dt}\right) = \Psi\left[\left(-\frac{1}{T_s}\right)\Psi\right] \qquad (29)$$

Consequently we have:

$$\frac{dV_L}{dt} = \left(-\frac{1}{T_s}\right)\Psi^2 \le 0 \qquad (30)$$

## 5. Results and discussions

In this section we show the two parts of our work, which in the first we present the validation by simulation of the synergetic approach and the second part gives the experimental results.

### 5. 1. Simulation results

Simulation results for SP75 PV module are presented, whose specifications are stated in Table 1.

*Table 1. Specification of PV array panel SP75*

| **Parameter** | **Value** |
|---|---|
| Maximum output power $P_{max}$ | 75W |
| Open circuit voltage $V_{oc}$ | 21.7 (V) |
| Short circuit current $I_{scr}$ | 4.8 (A) |
| Short circuit current temperature coefficient $K_i$ | 2.06 (mA/°C) |

The specification of the MPPT system used in the simulation and in the experimentation and shown in figure.6 is tabulated in Table 2.

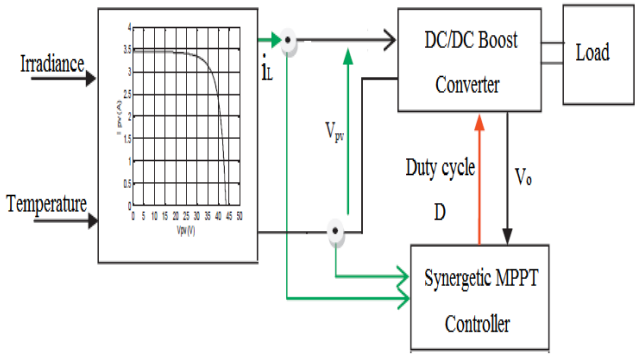


*Fig. 6. Proposed schematic system.*

*Table 2. System specification*

| Parameter | Value | Parameter | Value |
|---|---|---|---|
| $C$ | 220 ($uF$) | $q$ | 1.6 x $10^{-19}$ ($C$) |
| $L$ | 440 ($mH$) | $E_g$ | 1.12 ($eV$) |
| $T_s$ | 0.003 | $k_b$ | 1.38x$10^{-23}$ ($J/K$) |
| $T_r$ | 298 ($K$) | | |
| $R_L$ | 23Ω | | |

To show the effectiveness of the proposed control algorithm, the PV system is modeled and simulated using Matlab/Simulink environment.

The proposed MPPT is evaluated from two aspects: robustness to irradiance and temperature variation. In each figures, two different values of irradiance or temperature are presented in order to show the robustness.

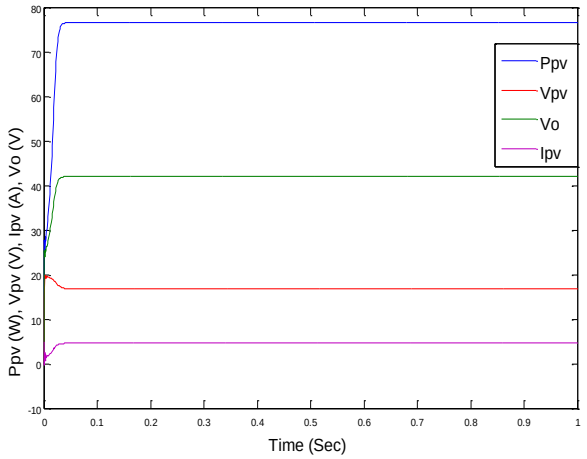


*(a)*

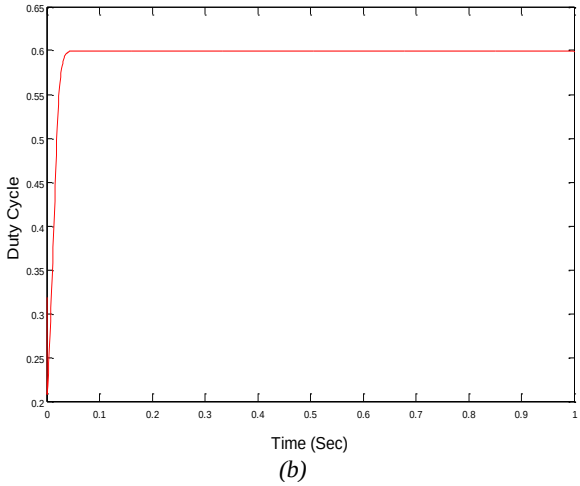


*(b)*

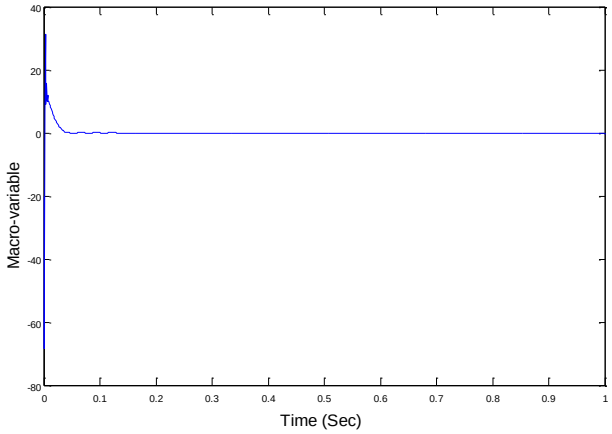


*(c)*

*Fig. 7. Simulation with standard condition: S=1000 W/m², T = 298 K*
*(a) $P_{pv}$,$V_{pv}$, $I_{pv}$ ,$V_o$ , (b) duty cycle , and (c) macro-variable.*

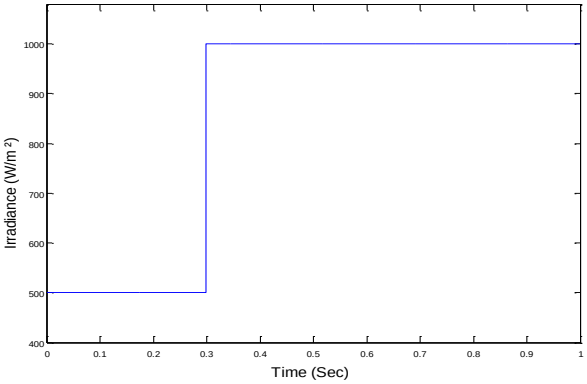


*Fig. 8. Solar irradiance variation.*

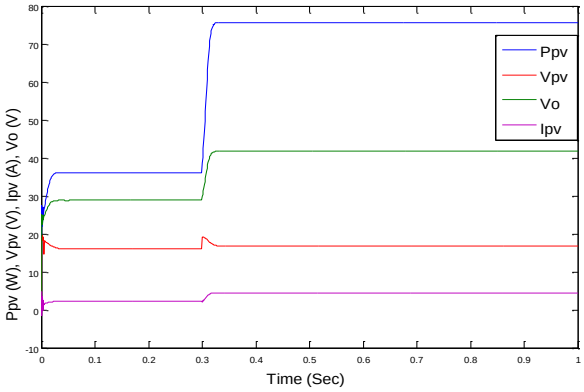


*(a)*

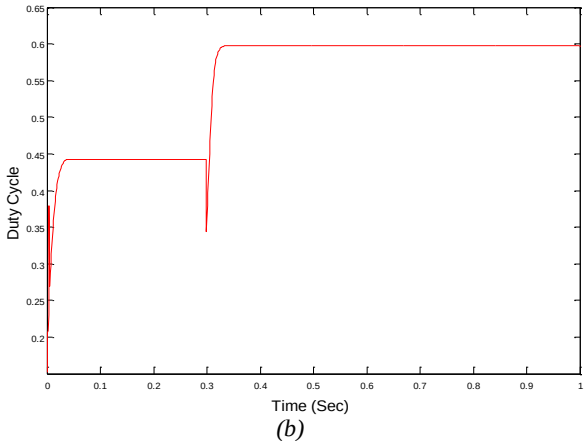


*(b)*

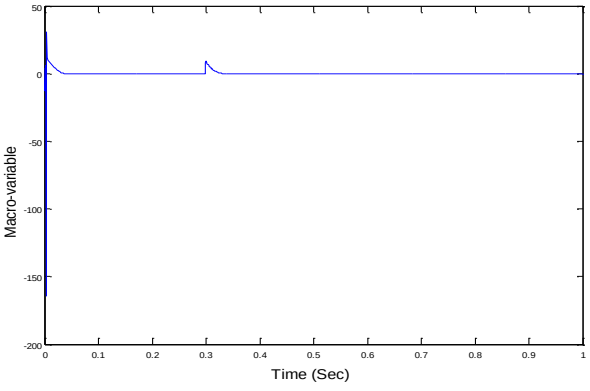


*(c)*

*Fig. 9. Simulation with step irradiance change (500 →1000 W/m², T = 298 K).*
*(a) $P_{pv}$,$V_{pv}$, $I_{pv}$ ,$V_o$ , (b) duty cycle , and (c) macro-variable.*

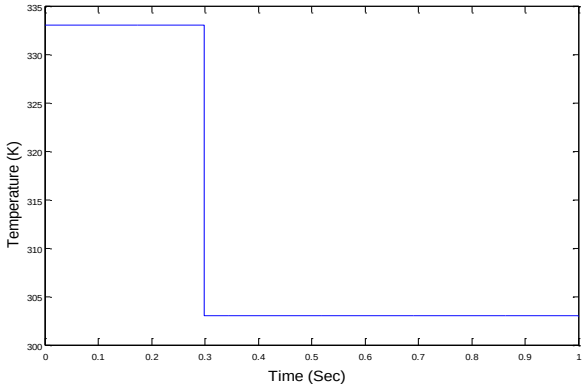


*Fig. 10. Temperature's variation.*

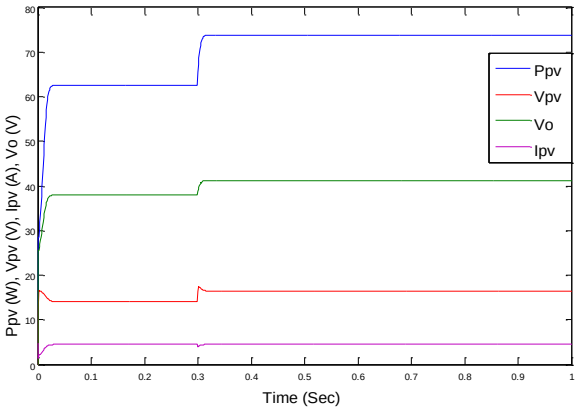


*(a)*

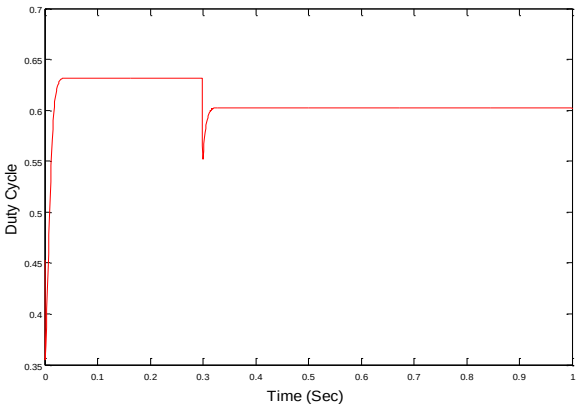


*(b)*

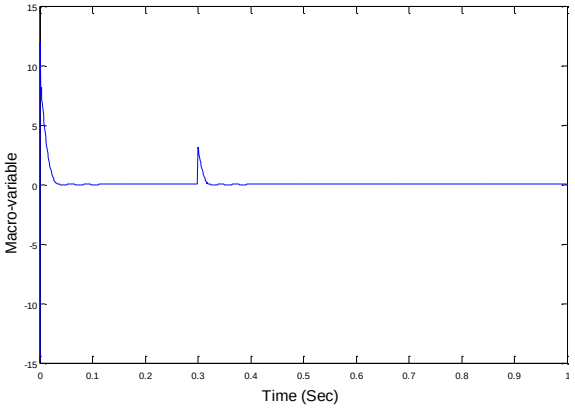


*(c)*

*Fig. 11. Simulation with step temperature change. (333 →303K, S= 1000 W/m²).*
*(a) $P_{pv}$,$V_{pv}$, $I_{pv}$ ,$V_o$ , (b) duty cycle , and (c) macro-variable.*

Fig. 7 shows the tracking result at Standard Test Condition: Irradiance = 1000W/m² and module temperature = 298K. Fig. 8 shows the solar irradiance variation.

Fig. 9 shows the tracking result at the changing irradiance level from 500 W/m² to 1000 W/m².

As shown in Fig. 9, when the irradiance level sharply changes at time 0.3s, the MPPT controller can track quickly the maximum power point.

Fig. 10 shows the temperature's variation.

Fig. 11 illustrates the system response under rapid temperature change from 333K to 303K. The system reaches steady state of both temperature levels within the order of milliseconds.

For all the simulation results above, the synergetic control approach is able to maintain the output at optimum point rapidly and provide high robustness to the variation of the external conditions.

### 5. 2. Experimental results

➢ **Experimental procedure**

The PV system under study and the complete automated test bench are presented in figure 12.This system comprises:

- PV modules providing 300 W of electrical power. Every panel is constituted by 36 PV cells and can deliver in the standard conditions of test (CST) a power of 60 W, a current of 4.4 A and a voltage of 13.2V [20-21]. Because, the functioning base of our algorithm are the electrical characteristics of the PV panels (Voltage, current and power), then we modeled in a fine way these characteristics according to weather conditions (illumination and the temperature) and data of the manufacturer.

- DC/DC Boost converter, whose role by using a digital MPPT control to match the PV Panels through the load. These converters functioning have been designed to work in continuous regime, with a hashing frequency of 10 KHz and dimensioned for a power of the order of 200 W [22-23].

- The implement digital MPPT controller, a PIC16F877 microcontroller as illustrated in figure 13, generates, according to the MPPT algorithm, a variable duty cycle PWM signal at 10 kHz and hence allows the PV system to converge to the maximal power point.

*Fig. 12. PV panels type SP75, test bench used in the laboratory, DC/DC Boost converter and digital MPPT control.*

The DC-DC Boost converter and the designed digital MPPT control are shown in fig. 13.

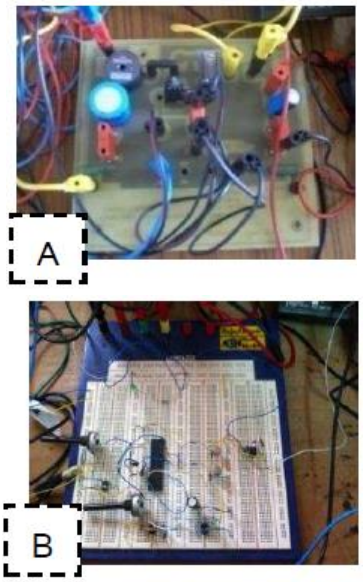


*Fig. 13. Cards realized in LETAS laboratory: (A) DC-DC converter (Boost), (B) Digital MPPT control.*

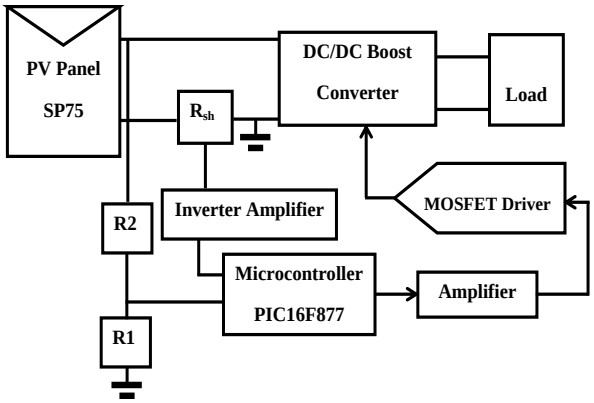


*Fig. 14. Synoptic diagram of the PV system equipped with the digital MPPT control.*

The synoptic diagram of the PV system equipped with the digital MPPT control is presented in figure (14).

To validate the new approach, the PV system is exposed to the solar radiation intensity varying from 730 W/m² to 765 W/m² at 34 °C. The parameters of the boost converter are L=440µH, C=220µF, and the load is a resistor of 23Ω.

On the fig. 15, the experimental electrical quantities of the PV panel and the simulated values corresponding to the maximum power point (power, voltage, current, duty cycle and macro-variable) are presented.

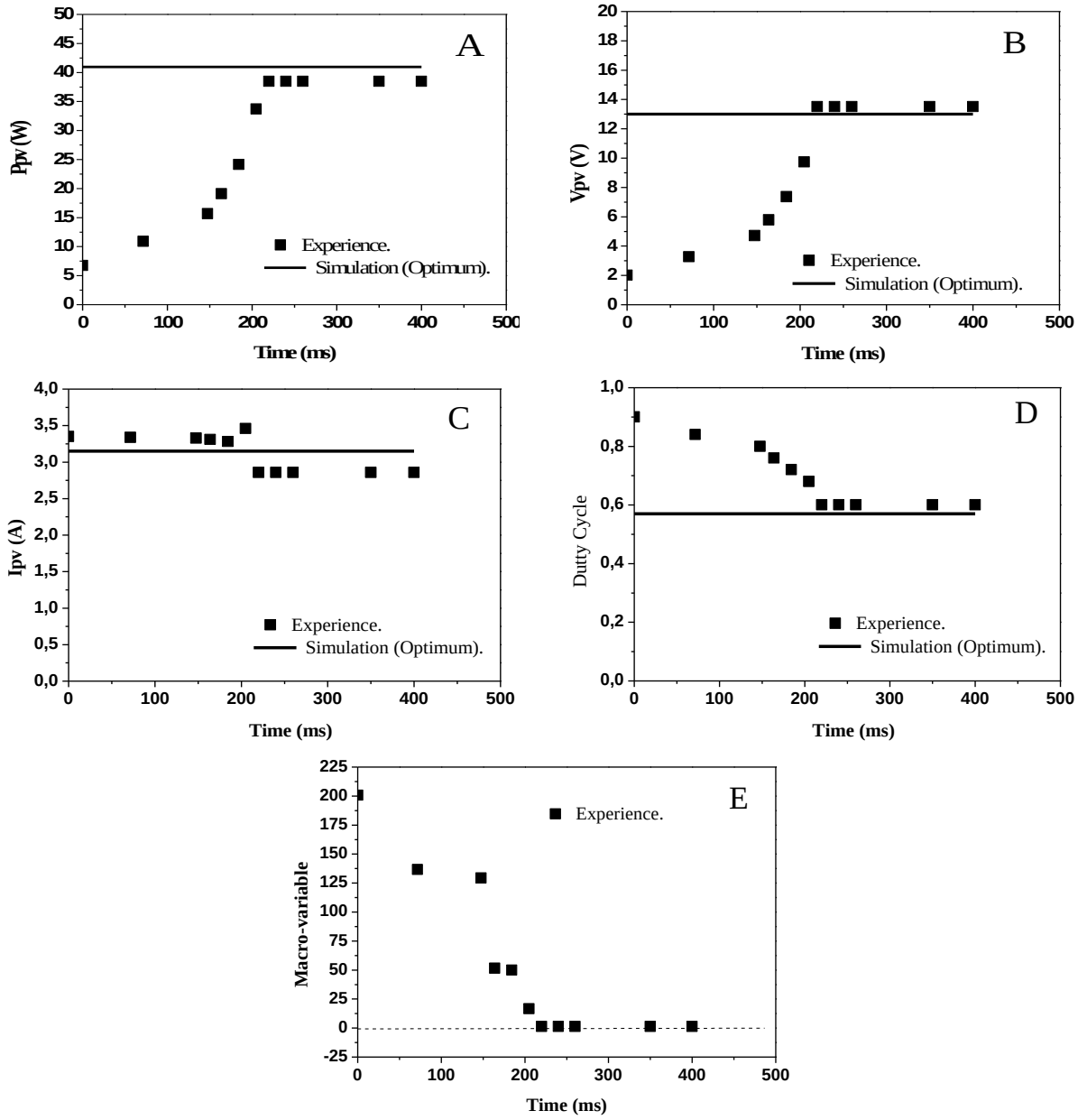


*Fig.15. Experimental and simulated (optimum) of electrical quantities of the PV system: (A) Power, (B) Voltage, (C) Current, (D) Duty cycle, and (E) macro-variable.*

The obtained experimental results show:

- A very good agreement between experiment and simulation results.

The synergetic PV system has been driven to the maximum value 40.95W at 200 ms by the synergetic controller (figure 15.(A))

- The voltage value after 200 ms is approximately 13V and the current effectively oscillate around the optimal 3.15 A value (figs. 15.(B) and 15.(C) respectively)

- The 0.57 duty cycle value which allowed us to reach the MPP at 200 ms is showed in the figure 15. (D) with a macro variable converging to near zero (fig. 15. (E)).

All the obtained experimental results show the validity of our approach, and the good functioning of the PV systems equipped with the digital MPPT synergetic control.

## 6. Conclusion

In this paper a new MPPT control strategy based on the synergetic control theory has been developed. The proposed controller is able to achieve the maximum power point under different temperatures and solar irradiances for photovoltaic systems.

This system is mainly composed of a solar array, DC/DC boost converter, synergetic MPPT controller, and an output load. The stability of the closed-loop system is guaranteed using the Lyapunov synthesis.

Both simulation in MATLAB/Simulink and experimental results are presented to validate the efficacy of this proposed approach, thus the obtained simulation results clearly demonstrate that the synergetic MPPT controller provides effective tracking of Maximum Power Point. Therefore, the simulation results confirm the validity of the synergetic control approach and its robustness to the variation of external conditions.

The experimental results validate the proposed synergetic approach and give a satisfactory results compared with those obtained by simulation.

## References

[1] L. A. C. Lopes, A. M. Lienhardt, Power Electronics Specialist, 2003.PESC'03. IEEE 34th Annual Conference on, Vol. 4, p. 1729, June 2003.
[2] M. A. S. Masoum, H. Dehbonei, E. F. Fuchs, IEEE Trans. Energy Convers., **17**(4), 514(2002).
[3] T. Esram, P. L. Chapman, IEEE Trans. Energy Convers., **22(**2), p. 439(2007).
[4] N. Femia, G. Petrone, G. Spagnuolo, M. Vitelli, IEEE Trans. Power Electron., **20**(4), pp. 963-973, Jul. 2005
[5] E. Koutroulis, K. Kalaitzakis, N. C. Voulgaris, IEEE Trans. Power Electron., 16(1), 46(2001).
[6] K. H. Hussein, I. Muta, T. Hoshino, M. Osakada, IEE Proc. Generation, Transmission and Distribution, **142**, 59(1995).
[7] S. Jain, V. Agarwal, Energy Conversion and Management, **48**, 625(2007).
[8] S. Kim, Solar Energy, **81**, 405(2007).
[9] H. Chih-Lyang, C. Li-Jui, Y. Yuan-Sheng, IEEE Transactions on Industrial Electronics, **54**, 574(2007).
[10] T. A. Venelinov, C. G. Leonardo, G. Vincenzo, C. Francesco, K. Okyay, IEEE Transactions on Industrial Electronics, **54**, 671(2007).
[11] Ch. Ben Salah, M. Chaaben, M. Ben Ammar, Renewable Energy, **33**, 993(2008).
[12] S.A. Kalogirou, Renewable and Sustainable Energy Reviews, **5**, 373(2001).
[13] B. Leger, J.B. Lopez-Velasco, J.M. Emidio, International Journal of Thermal Sciences, **41**, 1089(2002).
[14] N. Ould Cherchali, M.S. Boucherit, A. Morsli, L. Barazane, Journal of Electrical and Electronics Engineering, **7**(1), 117(2014).
[15] A. Kolesnikov, G. Veselov, A. Kolesnikov, et al. "Modern applied control theory: Synergetic Approach in Control Theory," vol. 2. (in Russian) Moscow – Taganrog, TSURE press, 2000.
[16] A. Kolesnikov, G. Veselov, A. Monti, F. Ponci, E. Santi, R. Dougal, in Proc. 17th Annual IEEE APEC, Dallas, TX, **1**, 409(2002).
[17] E. Santi, A. Monti, D. Li, K. Proddutur, R. Dougal, in Proc. 37th IEEE IAS Annual Meeting, **2**, 1330(2002).
[18] D. Li, K. Proddutur, E. Santi, A. Monti, in Proc. IEEE Southeast Conf., p. 197, Apr. 2002.
[19] Z. Bouchama M. Harmas, "Optimal robust adaptive fuzzy synergetic power system stabilizer design," Electr. Power Syst. Res, 2011.
[20] T. Mrabti, M. EL Ouariachi, K. Kassmi, B. Tidhaf. Moroccan Journal of Condenser Matter MJCM, Morocco, 12, 7(2010).
[21] T. Mrabti, M. El Ouariachi, R. Malek, Ka. Kassmi, B. Tidhaf, F. Bagui, F. Olivié, K. Kassmi, International Journal of Physical Sciences, **6**(35), 7865(2011).
[22] E. Baghaz, M. Melhaoui, M. F. Yaden, K. Kassmi, Physical Review & Research International, **4**(1), 80(2014).
[23] M.F. Yaden, M. Melhaoui, R. Gaamouche, K. Hirech, E. Baghaz, K. Kassmi, Electronics, **2**(3), 192(2013).

*Corresponding author: attoui_hadjira@yahoo.fr